JACS
JOURNAL OF THE AMERICAN CHEMICAL SOCIETY

Communication

pubs.acs.org/JACS

A Self-Assembled Cofacial Cobalt Porphyrin Prism for Oxygen Reduction Catalysis

Amanda N. Oldacre, Alan E. Friedman, and Timothy R. Cook*

Department of Chemistry, University at Buffalo, The State University of New York, Buffalo, New York 14260, United States

Supporting Information

ABSTRACT: Herein we report the first study of the oxygen reduction reaction (ORR) catalyzed by a cofacial porphyrin scaffold accessed in high yield (overall 53%) using coordination-driven self-assembly with no chromatographic purification steps. The ORR activity was investigated using chemical and electrochemical techniques on monomeric cobalt(II) tetra(*meso*-4-pyridyl)-porphyrinate (**CoTPyP**) and its cofacial analogue $[Ru_8(\eta^6\text{-}i\text{PrC}_6H_4Me)_8(dhbq)_4(\textbf{CoTPyP})_2][OTf]_8$ (**Co Prism**) (dhbq = 2,5-dihydroxy-1,4-benzoquinato, OTf = triflate) as homogeneous oxygen reduction catalysts. **Co Prism** is obtained in one self-assembly step that organizes six total building blocks, two **CoTPyP** units and four arene−Ru clips, into a cofacial motif previously demonstrated with free-base, Zn(II), and Ni(II) porphyrins. Turnover frequencies (TOFs) from chemical reduction (66 vs 6 h^{-1}) and rate constants of overall homogeneous catalysis (k_{obs}) determined from rotating ring−disk experiments (1.1 vs 0.05 h^{-1}) establish a cofacial enhancement upon comparison of the activities of **Co Prism** and **CoTPyP**, respectively. Cyclic voltammetry was used to initially probe the electrochemical catalytic behavior. Rotating ring−disk electrode studies were completed to probe the Faradaic efficiency and obtain an estimate of the rate constant associated with the ORR.

The ability to efficiently activate small molecules, such as oxygen, is important because of the role that these substrates play in carbon-neutral energy schemes, for example within hydrogen fuel cells.[1] Efforts to mimic naturally occurring catalysts for the oxygen reduction reaction (ORR) have motivated the study of metalloporphyrin architectures.[2] Among these, cofacial systems have unique advantages over their monomeric analogues. The presence of two metals distributes redox and coordination number demands across two sites, a useful feature for multielectron reactions. Furthermore, a preorganization of the transition state of activation may occur, which is manifested in enhanced rates of catalysis and selectivity over monomeric porphyrins.[3] Because of these advantages, a small number of *covalently* tethered structures have been reported that demonstrate reactivity of relevance to the ORR.[3,4] Cofacial platforms are rare, in part because of the complex, multistep covalent syntheses required to link two porphyrin macrocycles together, typically resulting in low yields and time-consuming purifications. The synthesis of these functionally promising structures can be greatly simplified with the use of one-pot, coordination-driven self-assembly techniques, wherein metal−ligand bond formation drives formation of the complex.[5] Coordination-driven self-assembled complexes have been broadly applied toward biomedical applications,[6] in host−guest systems,[7] and for catalysis.[8] Pyridyl-functionalized metalloporphyrins can be assembled into a cofacial conformation using an arene−ruthenium clip that forces a coplanar arrangement of the two macrocycles by bridging the pendant pyridyl sites (Figure 1). The synthesis of cofacial Ni(II) and

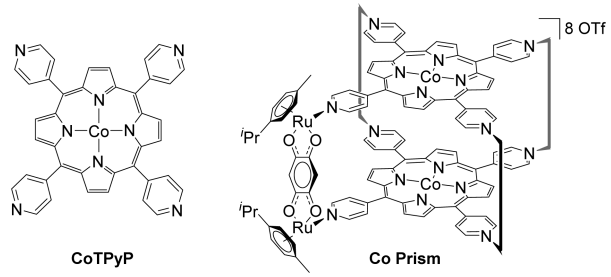

Figure 1. ORR catalysts cobalt(II) tetra(*meso*-4-pyridyl)porphyrinate (**CoTPyP**) and $[Ru_8(\eta^6\text{-}i\text{PrC}_6H_4Me)_8(dhbq)_4(\textbf{CoTPyP})_2][CF_3SO_3]_8$ (**Co Prism**).

Zn(II) porphyrin prisms has been established by Therrien and co-workers,[6c,9] and related self-assembled prisms are known.[10] Since the arene−ruthenium and porphyrin subunits are independently synthesized, the resultant cofacial complexes can be readily tuned without a total synthetic redesign, for example by altering the Ru−Ru distance within the clip or selecting an alternative metal in the porphyrin.[11] Herein we provide the first report of discrete self-assembled prisms that show catalytic activity for the ORR using a monomeric Co(II) porphyrin as a benchmark.

The arene ruthenium clip used for self-assembly is readily synthesized from the $\{Ru(\eta^6\text{-}i\text{PrC}_6H_4Me)(Cl)_2\}_2$ dimer and 2,5-dihydroxy-1,4-benzoquinone (H_2dhbq).[10a] The chlorides of the clip are removed prior to self-assembly by pretreatment with AgOTf, after which the appropriate porphyrin is added to the reaction vessel, as previously described in the literature for the Zn porphyrin used as a control in the current work.[9] The unreported Co(II) variant was obtained by initial formation of **CoTPyP** via a literature route followed by self-assembly conditions analogous to those for the Zn prism.[12] The metalation of TPyP with Co(II) was monitored by diagnostic

Received: December 1, 2016
Published: January 19, 2017

DOI: 10.1021/jacs.6b12404
J. Am. Chem. Soc. 2017, 139, 1424−1427

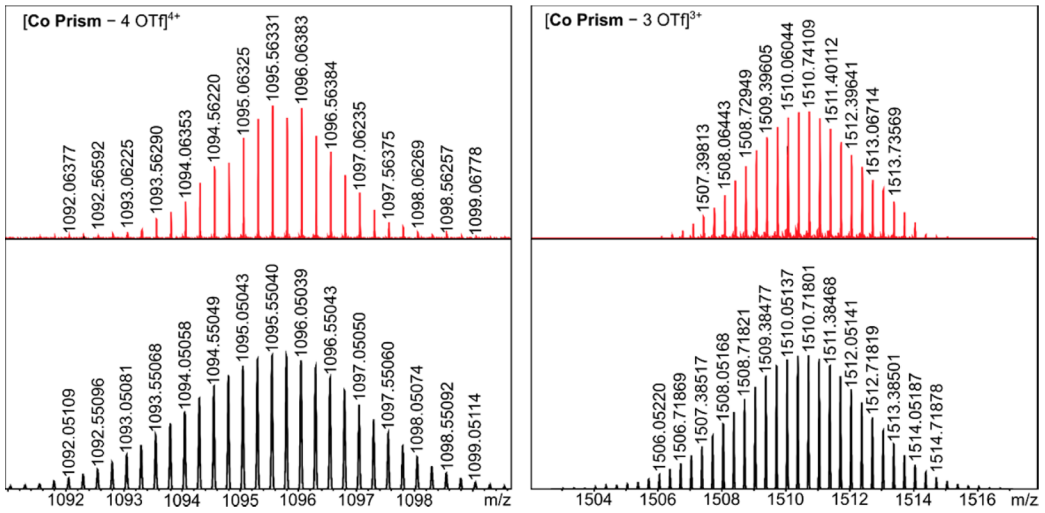

Figure 2. ESI-FTMS (red) and simulated (black) peaks corresponding to [**Co Prism** − 4OTf]$^{4+}$ (left) and [**Co Prism** − 3OTf]$^{3+}$ (right).

changes to the Q bands (collapsing to two bands from four) in the electronic absorption spectrum (see Figures S9 and S10). Evidence for the [2 + 4] stoichiometry of self-assembly was obtained from electrospray ionization mass spectrometry (ESI-FTMS). Two strong ion peaks were observed that correspond to intact **Co Prism** with a loss of three (m/z = 1510.74109) and four (m/z = 1095.56331) triflate counterions (Figure 2). The isotopic spacing of these peaks matches the simulated spectrum, providing strong evidence for the proposed structural assignment.

Oxygen reduction can deliver either H_2O or H_2O_2 via four-electron/four-proton or two-electron/two-proton pathways, respectively. Chemical reduction experiments may be used to determine the product distribution of homogeneous ORR catalysts using ferrocene (Fc) as an electron source, a method developed Fukuzumi and Guilard.[4b] In the absence of catalyst, no ferrocenium (Fc^+) was observed (λ = 620 nm) using oxygen-saturated PhCN and 100 mM trifluoroacetic acid (TFA) (see Figure S12). Figure 3 shows the concentration of Fc^+ formed over time in the presence of **CoTPyP** or **Co Prism**. No Fc^+ was formed using the Zn analogue of the prism (Figure S14). Under Fc-limiting conditions, the products of the ORR could be quantified. In the presence of **CoTPyP**, O_2, and TFA, Fc was completely oxidized to Fc^+ over the course of 7.5 h. A

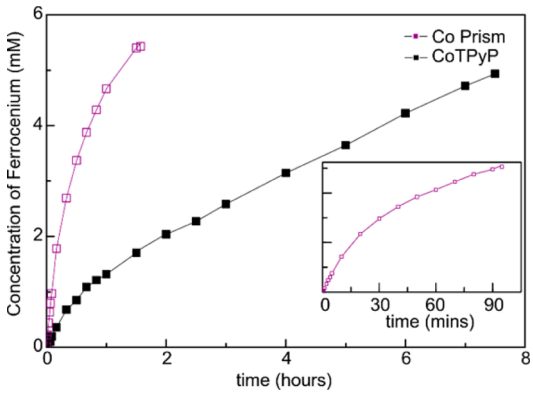

Figure 3. ORR catalysis by **CoTPyP** (0.04 mM, black), and **Co Prism** (0.02 mM, open purple) monitored by ferrocenium formation (λ_{max} = 620 nm) in oxygen-saturated PhCN and 100 mM TFA. The inset isolates the **Co Prism** data.

NaI titration was used to determine that 1.8 ± 0.064 mM H_2O_2 was produced over the course of the reaction.[4b] In the presence of **Co Prism**, O_2, and TFA, Fc oxidation to Fc^+ occurred over 1.5 h, and the NaI titration confirmed the production of 2.1 ± 0.083 mM H_2O_2. Under chemical reduction conditions, the selectivity (H_2O vs H_2O_2) and turnover frequency of **CoTPyP** and **Co Prism** are significantly different. The cobalt loading in each trial was normalized to 0.04 mM, and therefore, **Co Prism** displayed markedly increased kinetics over its monomeric counterpart, akin to previously observed cofacial enhancement.[3,13] However, **Co Prism** showed enhanced selectivity for H_2O_2 (90%) versus **CoTPyP** (70%). The apparent turnover frequency (TOF) for a given product[14] is defined as

$$\text{TOF} = \frac{\text{moles of product}}{(\text{moles of catalyst})(t)} \quad (1)$$

in which H_2O_2 is the product and t is the time (in hours). The turnover frequency for H_2O_2 of **Co Prism** (66 h^{-1}) is an order of magnitude greater than that of **CoTPyP** (6 h^{-1}).

The onset of catalysis for both **CoTPyP** and **Co Prism** occurs with a high overpotential, as no current response is observed until 0 V vs $Ag/AgNO_3$ is reached. Glassy carbon (GC) electrodes introduce background current past −0.6 V vs $Ag/AgNO_3$ and therefore obscure the catalysis at very reducing potentials. In previous reports it was shown that covalently bridged Co(II) porphyrin catalysts do not interact with O_2 in their neutral form and require preoxidation to enter ORR cycles, in stark contrast to monomeric systems, wherein no preoxidation is needed.[4c,15] Therefore, the effect of preoxidation on the activity of **CoTPyP** and **Co Prism** was investigated. The **CoTPyP** monomer interacts with O_2 and catalyzes oxygen reduction with no need for preoxidation (see Figure S25). No significant change to the current response is observed when initially scanning oxidizing versus reducing.

The same experiments were used to probe the effects of preoxidation on **Co Prism**. Figure 4 shows current responses that are dependent on the direction of the initial potential sweep. Although a strong oxidation feature is not observed when scanning toward anodic potentials, a significant change in current response occurs. The current response observed when the reducing potentials are applied first does not match that of **CoTPyP**, indicating that when reducing potentials are applied first, the activity is not due to each porphyrin simply acting like

DOI: 10.1021/jacs.6b12404
J. Am. Chem. Soc. 2017, 139, 1424−1427

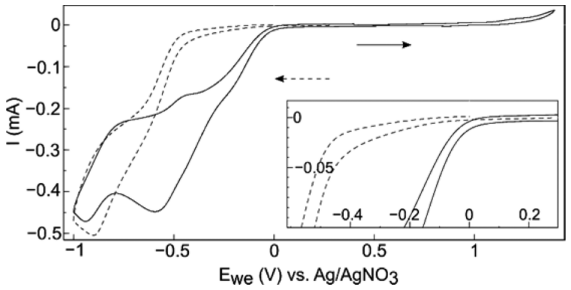

Figure 4. Cyclic voltammograms of 0.1 mM **Co Prism**, 100 mM $TBAPF_6$ (TBA = tetrabutylammonium), 100 mM TFA, and oxygen-saturated acetonitrile with initial scanning in the reducing (dashed) and oxidizing (solid) directions. The inset shows the onset potentials. Scan rate: 100 mV/s.

a monomeric site. Nonetheless, overpotentials are attenuated when preoxidation is performed.

Since catalysis by **CoTPyP** and **Co Prism** occurs with high overpotentials, it is possible for background current from the GC electrode to compete. Previous studies of **CoTPyP** indicate that it does not adsorb strongly on GC electrodes.[16] Thus, the current response associated with catalysis by **CoTPyP** and **Co Prism** can be corrected using porphyrin-free solutions (see Figure S33). The corrected current responses show plateau currents that can be used to estimate k_{obs}, associated with the overall rate of homogeneous catalysis,[17] using the methods of Savèant and co-workers.[18] From the rotating ring–disk electrode (RRDE) voltammograms, we can obtain product distributions (H_2O_2 vs H_2O) using the equation for Faradaic yield (eq 2):[19]

$$\%H_2O_2 = \frac{\frac{2i_{ring}}{N}}{i_{disk} + \frac{i_{ring}}{N}} \times 100 \qquad (2)$$

in which i_{ring} is the current response from the Pt ring, i_{disk} is the current response from the GC disk, and N is the collection efficiency of the RRDE. The collection efficiency was experimentally determined to be 0.35 (see Figure S1).[19a] Figure 5 shows the corrected RRDE current response of

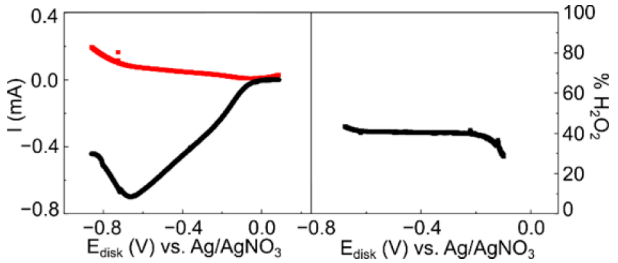

Figure 5. Corrected RRDE response (left) and Faradaic efficiency (right) of 0.2 mM **CoTPyP**, 100 mM $TBAPF_6$, 100 mM TFA, and oxygen-saturated acetonitrile. The Pt ring was held at 1.5 V vs Ag/$AgNO_3$. Rotation rate: 2500 rpm. $i_{pl} = 6.86 \times 10^{-4}$ A.

CoTPyP and its Faradaic efficiency. A plateau current (i_{pl}) is obtained at −0.6 V vs Ag/$AgNO_3$ and can be used to estimate k_{obs} only if the catalyst is not limited by mass transport.[18] k_{obs} can be estimated using eq 3:

$$i_{pl} = n_{ap}FAC^0_{cat}\sqrt{D_{cat}k_{obs}} \qquad (3)$$

in which n_{ap} is the apparent number of electrons transferred, F is the Faraday constant, A is the surface area of the electrode (0.95 cm^2), C^0_{cat} is the bulk concentration of the catalyst, D_{cat} is the diffusion coefficient of the catalyst, and k_{obs} is the apparent rate constant.[17,18] A D_{cat} of 1.1×10^{-5} cm^2/s was used with the assumption that the hydrodynamic radii of **CoTPyP** and ZnTPyP do not substantially differ. The diamagnetic nature of ZnTPyP enabled the determination of D_{cat} using DOSY NMR methods.[20] The n_{ap} value of 3.12 was calculated from eq 4:[18]

$$n_{ap} = 4 - 2\left(\frac{\%H_2O_2}{100}\right) \qquad (4)$$

The k_{obs} associated with catalysis by **CoTPyP** was calculated to be 0.05 h^{-1}.

Figure 6 shows the corrected RRDE current response of **Co Prism** and its Faradaic efficiency. A plateau current is obtained

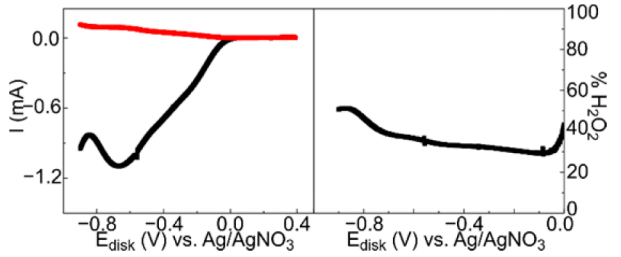

Figure 6. Corrected RRDE response (left) and Faradaic efficiency (right) of 0.1 mM **Co Prism**, 100 mM $TBAPF_6$, 100 mM TFA, and oxygen-saturated acetonitrile. The Pt ring was held at 1.5 V vs Ag/$AgNO_3$. Rotation rate: 2500 rpm. $i_{pl} = 1.03 \times 10^{-3}$ A.

at −0.7 Vvs Ag/$AgNO_3$. Equation 2 can also be applied to the **Co Prism** data using $D_{cat} = 4.1 \times 10^{-6}$ cm^2/s and $n_{ap} = 3.22$, revealing a k_{obs} of 1.1 h^{-1}. The D_{cat} used here was determined using a DOSY NMR measurement of the diamagnetic Zn Prism and an assumption that the paramagnetic **Co Prism** would have a similar hydrodynamic radius (see Figure S4). Since the concentration of Co sites was the same in both experiments, the increase in k_{obs} is attributed to a cofacial enhancement. The selectivities of **CoTPyP** and **Co Prism** are similar in the electrochemical studies, with average Faradaic efficiencies of 44% and 39%, respectively.

In conclusion, the first discrete self-assembled catalyst for oxygen reduction was synthesized in two facile steps using coordination-driven self-assembly in an overall yield of 53% without any need for purification by chromatography. This is a substantial improvement over traditional stepwise routes that are associated with overall yields of ∼3% or lower.[4c] **Co Prism** (66 h^{-1}) showed an enhanced turnover frequency over **CoTPyP** (6 h^{-1}) and catalyzed oxygen reduction to hydrogen peroxide almost exclusively (90%) in the chemical reduction studies. Electrochemical studies provided rate constants for the ORR using both the cofacial and monomeric catalysts. The selectivities of **CoTPyP** and **Co Prism** were similar in the electrochemical studies, with average Faradaic efficiencies for hydrogen peroxide of 44% and 39%, respectively. The cofacial enhancement is quite strong in this system, with the rate constant for **Co Prism** ($k_{obs} \approx 1.1$ h^{-1}) exceeding that of **CoTPyP** ($k_{obs} \approx 0.05$ h^{-1}) by over an order of magnitude. We have demonstrated herein that it is possible to realize the benefits of polynuclear catalysis using simple synthetic methods. Because the resulting molecules are obtained in high yields without tedious purification steps, we envision that a

DOI: 10.1021/jacs.6b12404
J. Am. Chem. Soc. 2017, 139, 1424–1427

library of such catalysts may now be rapidly populated. Toward this end, efforts are underway to exploit the modular nature of self-assembly using alternative building blocks that optimize the metal−metal separation, redox properties, and scaffold rigidity.

■ ASSOCIATED CONTENT

Supporting Information

The Supporting Information is available free of charge on the ACS Publications website at DOI: 10.1021/jacs.6b12404.

Experimental details, ^{1}NMR and DOSY spectra of Zn Prism, ESI-FTMS spectrum of **Co Prism**, UV−vis spectra, chemical reduction data, and cyclic voltammograms (PDF)

■ AUTHOR INFORMATION

Corresponding Author

*trcook@buffalo.edu

ORCID

Timothy R. Cook: 0000-0002-7668-8089

Notes

The authors declare no competing financial interest.

■ ACKNOWLEDGMENTS

T.R.C. thanks the University at Buffalo and the State University of New York Research Foundation for support. The project described was supported by Award S10RR029517 from the National Center for Research Resources.

■ REFERENCES

(1) Winter, M.; Brodd, R. J. *Chem. Rev.* **2004**, *104*, 4245.

(2) Yoshikawa, S.; Shimada, A. *Chem. Rev.* **2015**, *115*, 1936.

(3) Collman, J. P.; Wagenknecht, P. S.; Hutchison, J. E. *Angew. Chem., Int. Ed. Engl.* **1994**, *33*, 1537.

(4) (a) Devoille, A. M. J.; Love, J. B. *Dalton Trans.* **2012**, *41*, 65. (b) Fukuzumi, S.; Okamoto, K.; Gros, C. P.; Guilard, R. *J. Am. Chem. Soc.* **2004**, *126*, 10441. (c) Rosenthal, J.; Nocera, D. G. *Acc. Chem. Res.* **2007**, *40*, 543. (d) Chng, L. L.; Chang, C. J.; Nocera, D. G. *J. Org. Chem.* **2003**, *68*, 4075.

(5) (a) Cook, T. R.; Stang, P. J. *Chem. Rev.* **2015**, *115*, 7001. (b) Chakrabarty, R.; Mukherjee, P. S.; Stang, P. J. *Chem. Rev.* **2011**, *111*, 6810.

(6) (a) Cook, T. R.; Vajpayee, V.; Lee, M. H.; Stang, P. J.; Chi, K.-W. *Acc. Chem. Res.* **2013**, *46*, 2464. (b) Therrien, B. *Top. Curr. Chem.* **2011**, *319*, 35. (c) Barry, N. P. E.; Zava, O.; Dyson, P. J.; Therrien, B. *Aust. J. Chem.* **2010**, *63*, 1529.

(7) (a) Therrien, B. *Eur. J. Inorg. Chem.* **2009**, *2009*, 2445. (b) Maverick, A. W.; Billodeaux, D. R.; Ivie, M. L.; Fronczek, F. R.; Maverick, E. F. *J. Inclusion Phenom. Mol. Recognit. Chem.* **2001**, *39*, 19. (c) Nakamura, T.; Ube, H.; Shionoya, M. *Angew. Chem., Int. Ed.* **2013**, *52*, 12096. (d) Rousseaux, S. A. L.; Gong, J. Q.; Haver, R.; Odell, B.; Claridge, T. D. W.; Herz, L. M.; Anderson, H. L. *J. Am. Chem. Soc.* **2015**, *137*, 12713.

(8) (a) Catti, L.; Zhang, Q.; Tiefenbacher, K. *Chem. - Eur. J.* **2016**, *22*, 9060. (b) Koblenz, T. S.; Wassenaar, J.; Reek, J. N. H. *Chem. Soc. Rev.* **2008**, *37*, 247. (c) Meeuwissen, J.; Reek, J. N. H. *Nat. Chem.* **2010**, *2*, 615. (d) Davis, A. V.; Yeh, R. M.; Raymond, K. N. *Proc. Natl. Acad. Sci. U. S. A.* **2002**, *99*, 4793. (e) Howlader, P.; Das, P.; Zangrando, E.; Mukherjee, P. S. *J. Am. Chem. Soc.* **2016**, *138*, 1668. (f) Oliveri, C. G.; Gianneschi, N. C.; Nguyen, S. T.; Mirkin, C. A.; Stern, C. L.; Wawrzak, Z.; Pink, M. *J. Am. Chem. Soc.* **2006**, *128*, 16286.

(9) Barry, N. P. E.; Austeri, M.; Lacour, J.; Therrien, B. *Organometallics* **2009**, *28*, 4894.

(10) (a) Barry, N. P. E.; Govindaswamy, P.; Furrer, J.; Süss-Fink, G.; Therrien, B. *Inorg. Chem. Commun.* **2008**, *11*, 1300. (b) Shi, Y.; Sanchez-Molina, I.; Cao, C.; Cook, T. R.; Stang, P. J. *Proc. Natl. Acad. Sci. U. S. A.* **2014**, *111*, 9390. (c) Satake, A.; Kobuke, Y. *Tetrahedron* **2005**, *61*, 13. (d) Bar, A. K.; Mohapatra, S.; Zangrando, E.; Mukherjee, P. S. *Chem. - Eur. J.* **2012**, *18*, 9571.

(11) Cook, T. R.; Stang, P. J. Coordination-Driven Supramolecular Macromolecules via the Directional Bonding Approach. In *Hierarchical Macromolecular Structures: 60 Years after the Staudinger Nobel Prize I*; Percec, V., Ed.; Springer International Publishing: Cham, Switzerland, 2013; p 229.

(12) Nakazono, T.; Parent, A. R.; Sakai, K. *Chem. Commun.* **2013**, *49*, 6325.

(13) Chang, C. J.; Loh, Z.-H.; Shi, C.; Anson, F. C.; Nocera, D. G. *J. Am. Chem. Soc.* **2004**, *126*, 10013.

(14) Hartwig, J. F. *Organotransition Metal Chemistry: From Bonding to Catalysis*; University Science Books: Sausalito, CA, 2010.

(15) Le Mest, Y.; Inisan, C.; Laouénan, A.; L'Her, M.; Talarmin, J.; El Khalifa, M.; Saillard, J.-Y. *J. Am. Chem. Soc.* **1997**, *119*, 6095.

(16) Song, E.; Shi, C.; Anson, F. C. *Langmuir* **1998**, *14*, 4315.

(17) Rountree, E. S.; McCarthy, B. D.; Eisenhart, T. T.; Dempsey, J. L. *Inorg. Chem.* **2014**, *53*, 9983.

(18) Costentin, C.; Passard, G.; Savéant, J.-M. *J. Am. Chem. Soc.* **2015**, *137*, 5461.

(19) (a) Bard, A. J.; Faulkner, L. R. *Electrochemical Methods: Fundamentals and Applications*, 2nd ed.; Wiley: New York, 2001. (b) Passard, G.; Ullman, A. M.; Brodsky, C. N.; Nocera, D. G. *J. Am. Chem. Soc.* **2016**, *138*, 2925.

(20) Saiki, H.; Takami, K.; Tominaga, T. *Phys. Chem. Chem. Phys.* **1999**, *1*, 303.

DOI: 10.1021/jacs.6b12404
J. Am. Chem. Soc. 2017, 139, 1424−1427